Transmembrane peptides

DOI: 10.1002/anie.200705993

Effects of Guanidinium–Phosphate Hydrogen Bonding on the Membrane-Bound Structure and Activity of an Arginine-Rich Membrane Peptide from Solid-State NMR Spectroscopy

*Ming Tang, Alan J. Waring, Robert I. Lehrer, and Mei Hong**

Arginine- and lysine-rich cationic peptides and protein domains are found in a wide range of membrane-active proteins such as antimicrobial peptides,[1] cell-penetrating peptides,[2] and voltage-sensing domains of potassium channels.[3] Yet the three-dimensional structures these proteins adopt to enable translocation of the charged residues into the low dielectric milieu of the hydrophobic part of the lipid membrane, despite the free-energy barrier,[4] remain poorly understood. An increasing number of molecular dynamics simulations and experimental studies have suggested the importance of Arg interactions with lipids in membrane protein function.[5,6] Magic-angle spinning (MAS) solid-state NMR (SSNMR) spectroscopy can provide direct experimental insights into these intriguing questions of energetics and structure.

We have recently reported SSNMR distance-constrained guanidinium–phosphate ($Gdn–PO_4^-$) complex formation between the Arg residues of a β-hairpin antimicrobial peptide, PG-1, and the lipid phosphate groups.[7] The existence of these complexes suggests that the Arg residues are neutralized by the phosphate groups to enable transmembrane insertion of the peptide. We hypothesized that the peptide-associated phosphate headgroups transferred to the hydrophobic part of the membrane are responsible for the toroidal pore defects.[8] Such $Gdn–PO_4^-$ complexes should be stabilized by N–H···O=P hydrogen bonds and electrostatic attractions.[9]

Herein we test the importance of $Gdn–PO_4^-$ hydrogen bonding to the structure and activity of PG-1 by dimethylating each guanidinium group, thus reducing the number of N–H hydrogen-bond donors (Figure 1).[10] We show that this dimethylation of the Arg groups significantly alters the membrane insertion and activity of PG-1. Figure 2 shows oriented ^{31}P NMR spectra of palmitoyloleoylphosphatidylcholine/palmitoyloleoylphosphatidylglycerol (POPC/POPG) membranes containing 0–4% of the mutant (Arg^{mm}-PG-1).

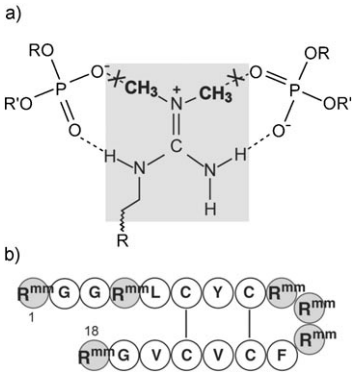

Figure 1. a) Structure of dimethylated Arg residue and its bidentate complex with phosphate ions. b) Arg^{mm}-PG-1 amino acid sequence.

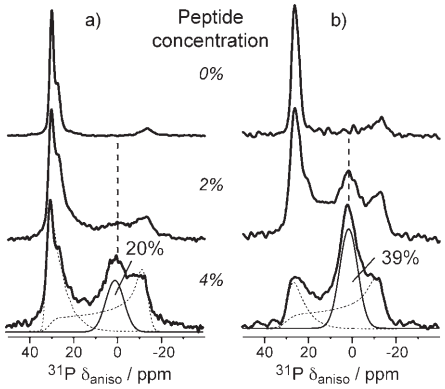

Figure 2. Oriented ^{31}P NMR spectra of POPC/POPG membranes with 0–4% a) Arg^{mm}-PG-1 and b) PG-1. The 4% sample spectra are simulated with an aligned peak, an isotropic peak, and a powder pattern, to yield the fraction of the isotropic peak.

Without the peptide, the membranes uniaxially aligned on glass plates and exhibited the expected single peak at approximately 30 ppm without other intensities in the anisotropic chemical shift range. Residual powder intensities indicative of misalignment and a small 0 ppm isotropic peak indicative of toroidal pores are observed with increasing concentrations of Arg^{mm}-PG-1. Line-shape simulations indicate that the isotropic component in the 4% Arg^{mm}-PG-1 sample is 20% of the total intensity, much less than the 39% caused by PG-1; thus, dimethylation of the Arg residues reduces membrane disruption.

Corroborating the ^{31}P NMR data are the minimal effective concentrations (MECs) of Arg^{mm}-PG-1 and PG-1 against

[*] M. Tang, Dr. M. Hong
Department of Chemistry, Iowa State University
Ames, IA 50011 (USA)
Fax: (+1) 515-294-0105
E-mail: mhong@iastate.edu
Homepage: http://www.public.iastate.edu/~hongweb
Dr. A. J. Waring, Dr. R. I. Lehrer
Department of Medicine
University of California at Los Angeles
Los Angeles, CA 90095 (USA)

Supporting information for this article is available on the WWW under http://www.angewandte.org or from the author.

a number of bacteria. In a solution containing salt concentrations similar to physiological levels, the average MEC of Arg^{mm}-PG-1 is 3.4-fold higher than PG-1, indicating that the mutant is 3.4-fold less potent (see the Supporting Information Table S1). At low salt concentration Arg^{mm}-PG-1 is still 1.4-fold less potent than PG-1. The weaker activity supports the lower membrane disorder of Arg^{mm}-PG-1 observed in the ^{31}P NMR spectra. The salt-concentration dependence of the two peptides suggests different mechanisms are involved in their antimicrobial action (see the Supporting Information).

To determine the topological structure of Arg^{mm}-PG-1 in the lipid membrane we measured the peptide–lipid ^{13}C–^{31}P distances. Figure 3 shows rotational echo double resonance (REDOR) distance curves of several ^{13}C-labeled sites. The Cα atom of L5, which is next to the most hydrophobic Arg residue, R4, increased its distance from 6.9 ± 1.6 Å in PG-1 to 8.5 Å in Arg^{mm}-PG-1, suggesting that the R4 mutation weakened the Gdn–PO_4^- complex. All measured distances are within 5.7–8.5 Å. Since the membrane has fewer isotropic defects in the presence of Arg^{mm}-PG-1 the distance similarity suggests that Arg^{mm}-PG-1 binds at the membrane/water interface, and the strand axis is roughly parallel to the membrane plane.

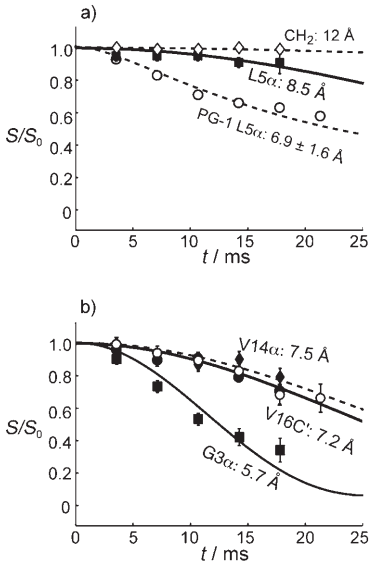

Figure 3. ^{13}C–^{31}P NMR distances of Arg^{mm}-PG-1 in hydrated POPE/POPG membranes. a) L5α (■) in Arg^{mm}-PG-1, compared with PG-1 (○). Lipid CH_2 data (◇) give the long distance limit. b) G3α (■) and V14α (◆) in Arg^{mm}-PG-1, and V16C′ in Arg^{mm}-PG-1 (●) and in PG-1 (○). S/S_0 is the intensity ratio of the REDOR dephasing spectrum with the control spectrum, measured with the ^{31}P pulses on and off, respectively.

We measured the distance between Arg^{mm}-PG-1 and the lipid chains by using a two-dimensional ^{31}P-detected ^1H spin diffusion experiment to verify the interfacial hypothesis.[11] In a peptide-free membrane the lipid chain $(CH_2)_n$ cross peak with the ^{31}P NMR signal is very weak because of the long distance and high mobility of the lipids. A rigid transmembrane (TM) peptide facilitates spin diffusion by its strongly coupled ^1H network, giving a high CH_2–P intensity. In contrast, a surface-bound peptide or a TM peptide with large-amplitude motion is an ineffective spin-diffusion conduit and produces low CH_2–P intensities.

The two-dimensional spectrum of Arg^{mm}-PG-1 in the POPE/POPG membrane at a mixing time of 64 ms is shown in Figure 4a. In the one-demensional cross sections the Arg^{mm}-PG-1 CH_2 intensity is higher than that of the pure membrane and lower than that of PG-1 (Figure 4b–d). The CH_2 build-up curves (Figure 4e) confirm that PG-1 has the fastest increase in intensity, as expected for the TM peptide; Arg^{mm}-PG-1 has a slower increase in intensity for the build-up curve, and the peptide-free bilayer has the smallest slope. These data support the interfacial binding of Arg^{mm}-PG-1.

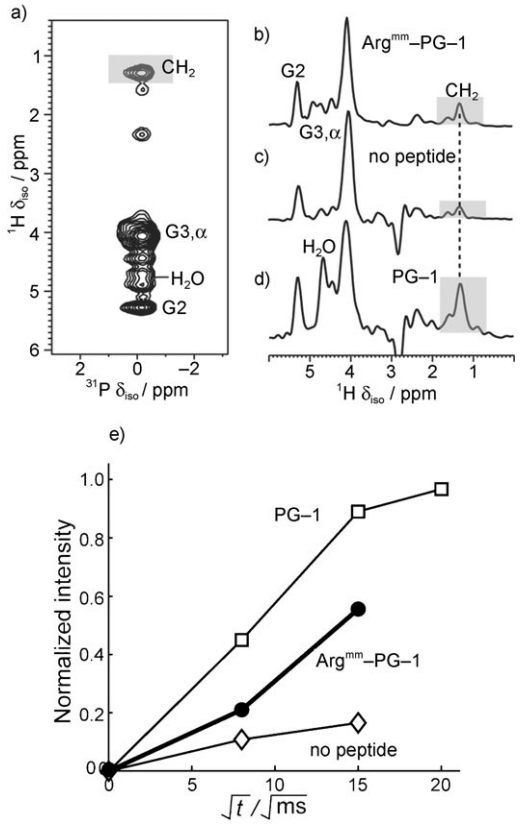

Figure 4. ^{31}P-detected ^1H spin diffusion spectra of POPE/POPG membranes at 303 K. a) 64 ms two-dimensional spectrum of Arg^{mm}-PG-1-containing membrane. b–d) 64 ms one-dimensional cross sections of membranes containing b) Arg^{mm}-PG-1, c) no peptide, and d) PG-1. e) CH_2 build-up curves for the three samples.

If Arg^{mm}-PG-1 is a TM peptide but highly mobile, it could still satisfy the ^1H spin diffusion data, therefore we measured C–H dipolar couplings of two Cα sites. Both L5 and V14 give Cα–Hα couplings that are 60–70% of the rigid-limit value in the POPC/POPG membrane (Table 1; and shown in two-dimensional Lee–Goldburg cross-polarization (LG-CP)[12] spectra in the Supporting Information, Figure S1), indicating that the peptide is mobile. This mobility contrasts with the fully immobilized PG-1 backbone in anionic membranes.[13,14] L5 and V14 are located next to disulfide bonds, thus backbone

Table 1: Cα $S_{Cα\text{-}Hα}$ values of Arg^{mm}-PG-1 in two anionic lipid membranes.

$S_{Cα\text{-}Hα}$	POPC/POPG	POPE/POPG
L5	0.69	0.84
V14	0.62	0.37

segmental motion is unlikely, and the reduced couplings are most likely because of rigid-body rotation of Arg^{mm}-PG-1 around the bilayer normal ($\vec{n}$). Indeed, recoupled Cα chemical shift anisotropies (CSA) of L5 and V14 show uniaxial line shapes (see the Supporting Information, Figure S2), confirming the uniaxiality of the backbone motion. Under this rotation, the $S_{Cα\text{-}Hα}$ value depends on the C–H bond orientation with respect to $\vec{n}$ as $S_{CH} = \langle(3\cos^2\theta - 1)/2\rangle$; the L5 and V14 $S_{Cα\text{-}Hα}$ values must be related by the orientations of the two bonds to each other and to $\vec{n}$, and therefore $S_{Cα\text{-}Hα}$ should indicate the peptide orientation.[15,16]

Calculated $S_{Cα\text{-}Hα}$ values for strand residues in an ideal antiparallel β-hairpin as a function of (τ, ρ) angles are shown (Figure 5 and the Supporting Information, S3 and S4):[17] τ is the tilt angle between the strand axis and $\vec{n}$ and ρ is the

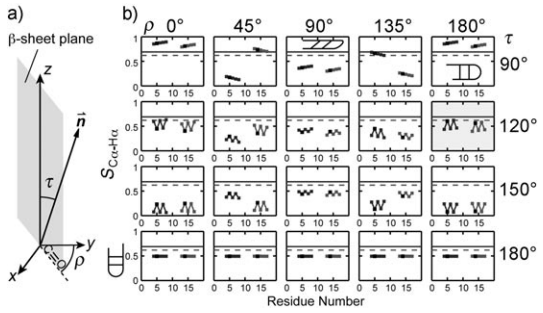

Figure 5. a) Definition of (τ, ρ) angles. τ is the angle between the strand axis *z* and the bilayer normal $\vec{n}$, and ρ is the angle between the C=O bond of residue six and the common plane of *z* and $\vec{n}$. b) Calculated $S_{Cα\text{-}Hα}$ of the strand residues (4–8 and 13–17) in an ideal β-hairpin as a function of (τ, ρ). The measured $S_{Cα\text{-}Hα}$ of L5 and V14 are drawn as solid and dashed lines, respectively. The best-fit (τ, ρ) panel, near (120°, 180°), is shaded.

rotation angle of the β-hairpin plane from $\vec{n}$. $\rho = 0°$ when $\vec{n}$ lies in the β-sheet plane. For the TM case $\tau \approx 180°$ and the $S_{Cα\text{-}Hα}$ value is generally less than 0.5 because the Cα–Hα bonds are close to being perpendicular to $\vec{n}$. For τ values of 130–180°, the calculated S_{CH} value is less than 0.6 for L5 and V14, which is inconsistent with the experimental data. As the strands become more parallel to the bilayer plane ($\tau \rightarrow 90°$), $S_{Cα\text{-}Hα}$ values become larger and vary over the entire range of 0–1. The best fit is when $\tau = 116°$ and $\rho = 179°$, indicating that the strand axis is roughly orthogonal to $\vec{n}$ and the hairpin plane is parallel to $\vec{n}$. The latter is reasonable because the peptide meets the least resistance in this orientation as it inserts into the membrane. Three other symmetry-related (τ, ρ) solutions exist, but they agree less well with the ^{13}C–^{31}P NMR distance data (see the Supporting Information, Table S2).

If residual segmental motion had remained at L5 and V14 Cα, it would mean that the whole-body $S_{Cα\text{-}Hα}$ value would be larger than 0.6–0.7, which would require τ to be even closer to 90°. Thus, the strand axis must be parallel to the membrane plane. In the POPE/POPG membrane, the L5 and V14 $S_{Cα\text{-}Hα}$ values change to 0.84 and 0.37, respectively (Table 1). The difference translates to only small (τ, ρ) changes, because of the high angular resolution of $S_{Cα\text{-}Hα}$ in this regime (see the Supporting Information, Figure S5), and the best fit is for τ at 113° and ρ at 164°. Thus, Arg^{mm}-PG-1 is interfacial in both anionic membranes. We also considered the effect of the backbone structure on the orientation calculation; the data show that even with the non-ideal PG-1 solution structure, the C–H dipolar couplings still constrain the strand axis to be perpendicular to $\vec{n}$ (see the Supporting Information, Figure S6 and Table S2).

Figure 6 summarizes the dramatic topology difference of Arg^{mm}-PG-1 and PG-1 in the lipid membrane. Compared to PG-1, the hydrogen bond deficient mutant is no longer a TM

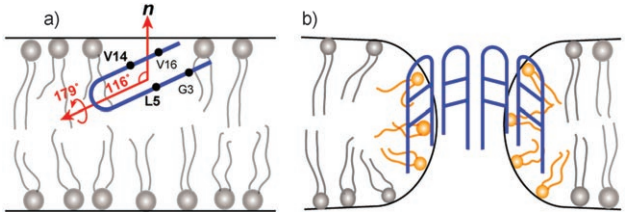

Figure 6. Topological structure of a) Arg^{mm}-PG-1 and b) PG-1 in anionic lipid membranes.

peptide, but is inserted to the membrane/water interface, 5.7–8.5 Å from the ^{31}P plane and further from the hydrophobic center of the membrane. The mutant is uniaxially mobile and thus not oligomerized, whereas PG-1 forms immobile multimeric β-barrels in the anionic membrane, possibly promoted by a high salt concentration. Thus, the reduction of hydrogen bonds caused by the dimethylation of the Arg residues in this antimicrobial peptide weakens Gdn–PO_4^- complexation, prevents peptide insertion and oligomerization, and reduces the disruptive activity of the peptide to the membrane. The data herein suggest that the remaining activity of Arg^{mm}-PG-1 is achieved by a different mechanism, most likely in-plane diffusion, which still gives rise to isotropic lipid morphologies, albeit at a lower level than the toroidal pore mechanism employed by wild-type PG-1.[18] Gdn–PO_4^- hydrogen bonding may also affect the structure and function of other Arg-rich membrane proteins, as suggested by recent molecular dynamics simulations of a potassium channel and a cell-penetrating peptide.[3,5,6]

Experimental Section

Arg^{mm}-PG-1 is synthesized by Fmoc chemistry and purified to greater than 95%. The peptides were reconstituted into lipid vesicles at a peptide/lipid molar ratio of 1:15. All NMR data were obtained at 9.4 Tesla by using a triple-resonance 4 mm MAS probe and a static probe. ^{13}C–^{31}P NMR REDOR experiments were conducted at 225 K

under 4.5 kHz MAS. Two-dimensional LG-CP and DIPSHIFT experiments were used to measure C–H dipolar couplings and the ROCSA experiment was used to measure the ^{13}C NMR CSA values. Further details of orientation simulations are given in the Supporting Information.

Received: December 30, 2007
Revised: February 12, 2008
Published online: March 13, 2008

Keywords: guanidinium ions · NMR spectroscopy · phospholipids · proteins · structure elucidation

[1] M. Zasloff, *Nature* **2002**, *415*, 389.
[2] R. Fischer, M. Fotin-Mleczek, H. Hufnagel, R. Brock, *ChemBioChem* **2005**, *6*, 2126.
[3] Y. Jiang, V. Ruta, J. Chen, A. Lee, R. MacKinnon, *Nature* **2003**, *423*, 42.
[4] T. Hessa, H. Kim, K. Bihlmaier, C. Lundin, J. Boekel, H. Andersson, I. Nilsson, S. H. White, G. von Heijne, *Nature* **2005**, *433*, 377.
[5] J. A. Freites, D. J. Tobias, G. von Heijne, S. H. White, *Proc. Natl. Acad. Sci. USA* **2005**, *102*, 15059.
[6] H. D. Herce, A. E. Garcia, *Proc. Natl. Acad. Sci. USA* **2007**, *104*, 20805.
[7] M. Tang, A. J. Waring, M. Hong, *J. Am. Chem. Soc.* **2007**, *129*, 11438.
[8] K. Matsuzaki, O. Murase, N. Fujii, K. Miyajima, *Biochemistry* **1996**, *35*, 11361.
[9] K. A. Schug, W. Lindner, *Chem. Rev.* **2005**, *105*, 67.
[10] J. B. Rothbard, T. C. Jessop, R. S. Lewis, B. A. Murray, P. A. Wender, *J. Am. Chem. Soc.* **2004**, *126*, 9506.
[11] D. Huster, X. L. Yao, M. Hong, *J. Am. Chem. Soc.* **2002**, *124*, 874.
[12] B. J. vanRossum, C. P. deGroot, V. Ladizhansky, S. Vega, H. J. M. deGroot, *J. Am. Chem. Soc.* **2000**, *122*, 3465.
[13] J. J. Buffy, A. J. Waring, R. I. Lehrer, M. Hong, *Biochemistry* **2003**, *42*, 13725.
[14] R. Mani, S. D. Cady, M. Tang, A. J. Waring, R. I. Lehrer, M. Hong, *Proc. Natl. Acad. Sci. USA* **2006**, *103*, 16242.
[15] M. Hong, T. Doherty, *Chem. Phys. Lett.* **2006**, *432*, 296.
[16] S. D. Cady, C. Goodman, C. Tatko, W. F. DeGrado, M. Hong, *J. Am. Chem. Soc.* **2007**, *129*, 5719.
[17] M. Tang, A. J. Waring, R. I. Lehrer, M. Hong, *Biophys. J.* **2006**, *90*, 3616.
[18] T. Doherty, A. J. Waring, M. Hong, *Biochemistry* **2008**, *47*, 1105.

